Long-Term and Seasonal Trends in Estuarine and Coastal Carbonate Systems
— **Source link** ↗

Jacob Carstensen, Melissa Chierici, Bo G. Gustafsson, Bo G. Gustafsson ...+1 more authors

Institutions: Aarhus University, University of Helsinki, Stockholm University

Related papers:

- Is Ocean Acidification an Open-Ocean Syndrome? Understanding Anthropogenic Impacts on Seawater pH

- Acidification of subsurface coastal waters enhanced by eutrophication

- Drivers of pH Variability in Coastal Ecosystems

- Standard potential of the reaction: , and and the standard acidity constant of the ion HSO4– in synthetic sea water from 273.15 to 318.15 K

- Coastal ocean acidification: The other eutrophication problem

Long-Term and Seasonal Trends in Estuarine and Coastal
Carbonate Systems

Carstensen, Jacob

2018-03

Key Points:
- Nutrient reduction can enhance coastal acidification with trends exceeding ocean acidification by factors ~2.5 for pH and ~4 for pCO_2
- Hydrological control can alter coastal carbonate chemistry more drastically than changing atmospheric CO_2, nutrient inputs, and temperature
- Coastal alkalinity behaves nonconservative due to calcifiers, nitrate assimilation, and anaerobic degradation processes in the sediments

Long-Term and Seasonal Trends in Estuarine and Coastal Carbonate Systems

Jacob Carstensen[1] ![iD], Melissa Chierici[2] ![iD], Bo G. Gustafsson[3,4] ![iD], and Erik Gustafsson[3] ![iD]

[1]Department of Bioscience, Aarhus University, Roskilde, Denmark, [2]Institute of Marine Research, Tromsø, Norway, [3]Baltic Nest Institute, Baltic Sea Centre, Stockholm University, Stockholm, Sweden, [4]Tvärminne Zoological Station, University of Helsinki, Hanko, Finland

Abstract Coastal pH and total alkalinity are regulated by a diverse range of local processes superimposed on global trends of warming and ocean acidification, yet few studies have investigated the relative importance of different processes for coastal acidification. We describe long-term (1972–2016) and seasonal trends in the carbonate system of three Danish coastal systems demonstrating that hydrological modification, changes in nutrient inputs from land, and presence/absence of calcifiers can drastically alter carbonate chemistry. Total alkalinity was mainly governed by conservative mixing of freshwater (0.73–5.17 mmol kg^{-1}) with outer boundary concentrations (~2–2.4 mmol kg^{-1}), modulated seasonally and spatially (~0.1–0.2 mmol kg^{-1}) by calcifiers. Nitrate assimilation by primary production, denitrification, and sulfate reduction increased total alkalinity by almost 0.6 mmol kg^{-1} in the most eutrophic system during a period without calcifiers. Trends in pH ranged from −0.0088 $year^{-1}$ to 0.021 $year^{-1}$, the more extreme of these mainly driven by salinity changes in a sluice-controlled lagoon. Temperature increased 0.05°C yr^{-1} across all three systems, which directly accounted for a pH decrease of 0.0008 $year^{-1}$. Accounting for mixing, salinity, and temperature effects on dissociation and solubility constants, the resulting pH decline (0.0040 $year^{-1}$) was about twice the ocean trend, emphasizing the effect of nutrient management on primary production and coastal acidification. Coastal pCO_2 increased ~4 times more rapidly than ocean rates, enhancing CO_2 emissions to the atmosphere. Indeed, coastal systems undergo more drastic changes than the ocean and coastal acidification trends are substantially enhanced from nutrient reductions to address coastal eutrophication.

1. Introduction

The global average CO_2 level in the atmosphere has risen from a preindustrial 280 ppm to approximately 400 ppm in 2016, resulting mainly from fossil fuel combustion, cement production, and land use change. Approximately 25% of the anthropogenic CO_2 emissions are currently absorbed by oceans (Le Quéré et al., 2016), which has resulted in an estimated global average surface water pH decline by ~0.1 unit over the last century (Caldeira & Wickett, 2003; Fietzke et al., 2015), a process commonly referred to as ocean acidification. Depending on the magnitude of future CO_2 emissions, pH is expected to further decrease by some 0.3–0.4 unit before the year 2100 (Orr et al., 2005). Long-term observations of ocean surface waters show an annual CO_2 increase of about 2 ppm, which corresponds to the rate of change in the atmosphere and converts to a current decadal pH decrease of about 0.02 (Doney, 2010; Olafsson et al., 2009).

While a gradual decrease in pH is a predictable open-ocean response to elevated anthropogenic CO_2 emissions, pH changes and long-term trends in coastal seas are usually considerably more complex (Duarte et al., 2013). In coastal ecosystems, pH can, in particular on a seasonal scale, be highly influenced by changes in nutrient, total alkalinity (A_T) and organic matter inputs from land, productivity, and respiration. For example, Melzner et al. (2013) reported seasonal changes in pH ranging ~0.6 pH unit for a coastal bay in the western Baltic Sea, that is, a seasonal signal much stronger than the expected centennial decline. Saderne et al. (2013) even reported diel pH variations in a range of 0.3–0.4 pH unit in nearshore macrophyte meadows of the western Baltic Sea. Understanding and describing seasonal changes in pH in coastal areas is a prerequisite to disentangling long-term trends.

If primary production is enhanced by excess nutrient inputs, one consequence is a simultaneous boost in surface water pH during the productive season because of increased CO_2 assimilation by phytoplankton. Oppositely, below the euphotic zone an increase in the supply of organic material causes an enhanced

CO_2 production through microbial respiration. Thus, eutrophication increases summertime pH in the productive layer and may at the same time induce subsurface acidification in coastal seas (Cai et al., 2011; Hagens et al., 2015; Melzner et al., 2013). However, anoxic degradation of organic material can counteract acidification through processes such as denitrification and burial of, for example, pyrite and vivianite—processes that result in a net increase of A_T and CO_2 buffering capacity (Reed et al., 2016; Thomas et al., 2009).

Riverine inputs of dissolved organic substances cause further changes in the acid-base balance of coastal seas for a couple of reasons. First, degradation of terrestrial organic carbon directly influences pH by releasing CO_2. Second, dissolved organic substances can, depending on composition and concentration, contribute significantly to A_T via the addition of organic alkalinity and in extension alter the CO_2 buffering capacity and pH (Ulfsbo et al., 2015). Acidic rain accompanying anthropogenic emissions of sulfur and nitrogen oxides (SO_x and NO_x) can further influence pH both directly via precipitation on the sea surface and indirectly by precipitation in the catchment area, which then affects weathering and cause long-term changes in the river loads of dissolved inorganic carbon (DIC) and A_T (Hjalmarsson et al., 2008; Müller et al., 2016; Omstedt et al., 2015).

In addition to the well-described ocean trends, long-term changes in pH and A_T have been reported for marginal seas such as the Baltic Sea (e.g., Beldowski et al., 2010; Müller et al., 2016). However, studies from coastal environments, where the carbonate system is more dynamic and complex (Borges & Gypens, 2010; Cai et al., 2011), are generally lacking. Nevertheless, decadal changes in pH can be as large as 0.4–0.6 pH unit for coastal systems that have experienced large changes in nutrient inputs (Duarte et al., 2013), that is, pH changes much larger than predicted from ocean acidification alone.

Many monitoring programs were established in Europe and North America during the 1970s and 1980s to assess changes in water quality variables associated with eutrophication, and trends in these variables covering almost half a decade have been reported (e.g., Carstensen et al., 2006; Kemp et al., 2005; Riemann et al., 2016). More recently, ocean and coastal acidification, and particularly the potential impacts it has on marine organisms, has gained increasing attention, although pH and A_T measurements are still not routinely monitored in most monitoring programs. Fortunately, long-term records of pH and A_T are available from some coastal monitoring programs, where they have been measured in connection with primary production or without any specific monitoring objective in mind. It must be stressed that these data are much more heterogeneously distributed in time and space, compared to the standard water quality variables.

In this study, we will investigate seasonal and long-term changes in pH and carbonate chemistry using monitoring data from three estuaries in Denmark that have all experienced large reductions in nutrient inputs and increases in temperature over the last 3–4 decades. Our aim is to demonstrate the potential for deriving such information from sparsely sampled data and to separate the long-term effects of increasing atmospheric CO_2, warming and oligotrophication on carbonate chemistry in coastal ecosystems.

2. Study Sites

We examined three coastal systems in Denmark (Figure 1) that have been intensively monitored over several decades as part of the Danish National Aquatic Monitoring and Assessment Program (DNAMAP) that was established to assess responses to nutrient management plans of reducing nitrogen and phosphorus inputs by 50% and 80%, respectively (Carstensen et al., 2006). Eutrophication in these coastal systems is primarily driven by nutrient inputs from land (Riemann et al., 2016) and all three systems have experienced reduced nutrient inputs from land over the last three decades (Figure S1 in the supporting information).

Although DNAMAP was mainly targeting nutrient and oxygen conditions as well as biological effects of eutrophication, occasionally, water samples were analyzed for pH and A_T as well. We also included data from regional monitoring programs established prior to DNAMAP. The three coastal systems are relatively shallow with mean depths ranging from 1.9 to 5.5 m and have comparable catchment and surface areas (Table 1). In all three catchments, agriculture is the dominant land use. However, soil characteristics of the three catchments were quite different with substantial effect on carbonate chemistry in the three coastal systems.

Ringkøbing Fjord is a coastal lagoon situated on the west coast of Denmark. The exchange with the North Sea is controlled by a sluice gate to prevent flooding of the lagoon's catchment. The surrounding landscape is mostly flat, and the lagoon is strongly exposed to winds, predominantly coming from westerly directions.

Figure 1. The three studied coastal systems with locations of the marine monitoring stations. Monitoring stations representing the outer boundary are marked in red and catchments are indicated with darker color.

Due to the strong influence of winds, the water column is usually mixed to the bottom. The lagoon underwent a regime shift around 1996 from turbid conditions with high phytoplankton biomass (dominated by cyanobacteria) to clearer conditions with benthic filter feeders controlling the algae (Petersen et al., 2008). The regime shift was induced by a change in the sluice gate operation that raised salinity and allowed the suspension-feeding clam *Mya arenaria* to settle in the lagoon. Freshwater inputs are dominated by the river Skjern Å, which drains ~80% of the entire catchment. The lagoon and catchment were beyond the ice front during the last glaciation period, and consequently, sandy soils dominate.

Roskilde Fjord is a long-stretched estuary with many small streams discharging along the entire course. It has two broads connected with a channel, where the inner broad is mostly mixed whereas the outer and somewhat deeper broad experience periods of stratification. The outer broad is connected to the Kattegat through a narrow strait. The estuary displays a distinct salinity gradient ranging from 10–15 in the southern broad to 15–20 in the northern broad. High densities of blue mussels (*Mytilus edulis*) throughout the estuary exert strong top-down control on phytoplankton. The landscape surrounding Roskilde Fjord is moraine with clay and organic-rich soils.

Skive Fjord, which here also includes the neighboring Hjarbæk Fjord, Lovns Bredning, and Riisgaarde Bredning, is the innermost part of the Limfjorden estuarine complex. Saline water from the North Sea enters Skive Fjord through the outer parts of Limfjorden as a bottom current creating stratified conditions that are

Table 1
Physical Characteristics of the Three Danish Coastal Systems With the Number of pH and A_T Measurements Used in the Study

Estuary	Catchment area (km^2)	Surface area (km^2)	Mean depth (m)	Max depth (m)	Residence time (day)	# of pH obs.	# of A_T obs.
Ringkøbing Fjord	3,475	283	1.9	5.1	127	1,483	1,548
Roskilde Fjord	1,176	124	3.0	30.7	90	2,181	277
Skive Fjord	2,621	248	5.5	23.9	100	6,512	1,811

Note. Water residence times, calculated for winter maximum freshwater discharge, are from Josefson and Rasmussen (2004).

intermittently broken down by winds. Hypoxia develops episodically during summer because of stratified conditions and high nutrient inputs from land. Mussel beds (*Mytilus edulis*) form on the shallower shoals and are regularly harvested by dredging. Freshwater inputs are dominated by a few large streams discharging into the southern parts of the coastal system. Salinity gradients are strong, particularly in the eastern branch (Hjarbæk Fjord). Catchment soils are a mix of sand, clay, and moraine.

3. Materials and Methods

Our aim is twofold: (1) to describe observed changes in the carbonate system over time and (2) to disentangle effects of eutrophication, increasing atmospheric CO_2 and warming on the carbonate system after accounting for estuarine mixing and carbonate speciation from varying salinity and temperature. Estuaries are characterized by intense mixing of fresh and marine waters, and we used data from these end-members to describe conservative mixing across the land-sea gradient. A_T was not measured as frequently as pH, and for calculating a more complete data set on carbonate chemistry, we predicted A_T from a statistical model that described spatial and temporal variations in addition to conservative mixing between the end-members. Furthermore, we assessed the potential effect on coastal calcifiers by calculating the saturation states (Ω) of $CaCO_3$. Long-term and seasonal trends were derived by partitioning variations in data among months and years of sampling as well as describing spatial variation. Long-term trends in annual means were tested by linear regression using the inverse variance of the mean estimate for weighting. Variation partitioning was performed using PROC GLM in SAS. Details are given below.

3.1. Carbonate System

Total DIC, partial pressure of carbon dioxide (pCO_2), and calcium carbonate saturation of aragonite ($\Omega_{Aragonite}$) and calcite ($\Omega_{Calcite}$) were calculated from observations of pH and A_T using the system of equations defining the carbonate system (Dickson, Sabine, & Christian, 2007). Measured pH (NBS scale) was translated to the total scale using Millero (1986). The contributions of phosphate, silica, and ammonium to A_T were not included in the equations, since these variables were not measured consistently with all A_T measurements and contribute marginally to A_T. We calculated CO_2 solubility constants (Weiss, 1974), CO_2 dissociation constants (Millero et al., 2006), water autodissociation constants (Millero, 1995), and sulfate and borate equilibrium constants (Dickson, 1990) as functions of salinity and temperature. Borate, sulfate, and fluoride concentrations were not measured but modeled proportional to salinity (Dickson et al., 2007). Saturation states for aragonite and calcite were computed using concentrations of CO_3^{2-} and dissolved calcium ions (Ca^{2+}) together with solubility constants calculated using Mucci (1983). Coastal Ca^{2+} concentrations were estimated by interpolating freshwater concentrations and ocean concentrations of 10 mmol L^{-1} using salinity. Calculated values of DIC, pCO_2, $\Omega_{Aragonite}$, and $\Omega_{Calcite}$ express conditions experienced in the estuarine environment. The carbonate system calculations were implemented as a SAS macro, which was validated against CO2SYS (Pierrot et al., 2006).

After calculating DIC from observed pH and A_T, we recalculated pH and pCO_2 for a standard salinity of 15 and temperature of 10°C (approximately average conditions for the three estuaries) by expressing A_T as function of DIC, borate, fluoride, and H^+ concentrations and solving this equation for H^+ using Newton-Raphson with dissociation and solubility constants calculated for standard salinity and temperature. Since dissociation and CO_2 solubility depends on salinity and temperature, these standardized values for pH and pCO_2 provide comparable data for assessing effects of biological processes, atmospheric pCO_2, and mixing on the carbonate system over time and across the three estuaries.

3.2. Freshwater Data

Stream pH, A_T, and Ca^{2+} in the three catchments were extracted from the DNAMAP database. All three variables were measured by standard methods: pH was measured with calibrated electrodes, A_T and Ca^{2+} by potentiometric titration. We used data from the regular stream monitoring stations: 10 in Ringkøbing Fjord catchment, 12 in Roskilde Fjord catchment, and 9 in Skive Fjord catchment. However, sampling for the three variables was relatively uneven over time and space. The upstream area of the monitoring stations varied from 1.2 to 2,316 km^2 in Ringkøbing Fjord catchment, from 0.84 to 257 km^2 in Roskilde Fjord catchment, and from 0.94 to 304 km^2 in Skive Fjord catchment. pH was most frequently measured with 18,271 observations in total (5,043 in Ringkøbing Fjord catchment, 7,078 in Roskilde Fjord catchment, and 6,150 in Skive

Fjord catchment), followed by A_T with 5,516 observations in total (2,714 in Ringkøbing Fjord catchment, 213 in Roskilde Fjord catchment, and 2,589 in Skive Fjord catchment), and Ca^{2+} with 794 observations in total (164 observations in Ringkøbing Fjord catchment, 425 observations in Roskilde Fjord catchment, and 205 observations in Skive Fjord catchment).

We analyzed measured pH, A_T, and Ca^{2+} in streams (denoted by X_{ijklm}) by partitioning variations into seasonal, interannual, and spatial components using the following model

$$X_{ijklm} = stream_i + station_j(stream_i) + year_k + month_l + e_{ijklm} \qquad (1)$$

where parameters $stream_i$ describe variation among streams (indexed by i), $station_j(stream_i)$ describe variation among monitoring stations within the same stream, $year_k$ describe variation among years with data, $month_l$ describe the seasonal variation using 12 monthly means, and e_{ijklm} is the residual error. Marginal means (mean of one factor averaged across all levels of other factors) for the interannual and seasonal variation were computed as weighted linear combinations of parameter estimates from the model. Estimates for $station_j(stream_i)$ were weighted by the area upstream of the monitoring stations and estimates for $stream_i$ were weighted by the stream catchment area, whereas parameter estimates for $month_l$ and $year_k$ were given equal weights. Hence, marginal means for $year_k$ represented means across all 12 months (equal weight) and all monitored streams (area-weighted), and similarly, marginal means for $month_l$ represented means across all years (equal weight) and all monitored streams (area-weighted).

3.3. Marine Data

Marine pH (NBS scale) and A_T as well as salinity and temperature were extracted from the DNAMAP database at 6 stations in Ringkøbing Fjord, 12 stations in Roskilde Fjord, and 12 stations in Skive Fjord (Figure 1). For each of the estuaries, one monitoring station was identified as representing boundary conditions for the system. Ca^{2+} was not measured in the marine monitoring program. Across the three coastal systems there were 9,791 pH measurements (Ringkøbing Fjord: 1,336, Roskilde Fjord: 2,860, Skive Fjord: 5,595) and 3,678 A_T measurements (Ringkøbing Fjord: 1,431, Roskilde Fjord: 445, Skive Fjord: 1,802). Discrete samples for pH and A_T were taken at varying depths from the surface down to 30 m in Roskilde Fjord. However, the majority of samples were from the top 5 m, representing the average water column as a whole (Table 1).

We analyzed variations in salinity, temperature, pH, A_T, DIC, CO_2 partial pressure (pCO_2), $\Omega_{Aragonite}$, and $\Omega_{Calcite}$ (denoted by Y_{ijklm}) for the three coastal systems, separating boundary stations and stations inside the coastal systems. Variations in Y_{ijklm} were partitioned into seasonal, interannual, and spatial variation using the following model

$$Y_{ijklm} = station_i + year_j + month_k + e_{ijl} \qquad (2)$$

where parameters $station_i$ describe the variation among monitoring stations, $year_j$ describe variations among years with data, $month_k$ describe the seasonal variation using 12 monthly means, and e_{ijl} is the residual error. Furthermore, this model was employed separately for the years before and after the regime shift in Ringkøbing Fjord (Petersen et al., 2008), because we expected that the seasonal variation could have changed. Marginal means for the interannual variation were calculated by averaging across parameter estimates for $station_i$ and $month_k$, and similarly for the marginal means describing the seasonal variation. These marginal means represent mean levels experienced by organisms in the coastal systems in a given year or month. DIC, pCO_2, $\Omega_{Aragonite}$, and $\Omega_{Calcite}$ displayed right-skewed tendencies and were log transformed before employing equation (2) and the mean values were back-transformed using the exponential function with bias correction to represent arithmetic means.

3.4. Accounting for Estuarine Mixing

Seasonal variations in the freshwater and outer boundary end-members were characterized by monthly means for salinity and relevant variables within the carbonate system. Conservative mixing within the estuary was defined by these end-members, yielding an expected value ($E[]$) of the concentration (C_t) for a given salinity S_t at a given time (t) as function of representative end-member concentrations (FW = freshwater, OB = outer boundary)

$$E[C_t | S_t] = C_{FW} - \frac{C_{FW} - C_{OB}}{S_{OB}} \cdot S_t \tag{3}$$

End-member concentrations were calculated as the average across all 12 months, since water residence times were at least 3 months for maximum freshwater discharge (Table 1) and probably >1 year during low freshwater discharge.

The prediction error (residual) from conservative mixing ($r_t = C_t - E[C_t | S_t]$) was analyzed for systematic temporal and spatial departures using a model similar to equation (2)

$$r_t = \mu + \text{station}_i + \text{year}_{j(t)} + \text{month}_{k(t)} + e_t \tag{4}$$

This model was used to predict A_T observations to supplement the more numerous pH observations by reconstructing values at a given time, location, and salinity as

$$\widehat{A}_T = E[C_t | S_t] + E\left[r_t | \text{station}_i, \text{year}_{j(t)}, \text{month}_{k(t)}\right] \tag{5}$$

and the marginal means of $\text{year}_{j(t)}$ and $\text{month}_{k(t)}$ in equation (4) were used to investigate long-term and seasonal trends in total alkalinity and other variables of the carbonate system, adjusting for conservative mixing. Thus, variations in r_t were primarily due to changes in atmospheric pCO$_2$ and biological processes, when accounting for mixing as well as temperature and salinity effects on dissociation and solubility constants.

4. Results

4.1. Characterizing End-Members of Estuarine Mixing

Observations of pH, A_T, and Ca^{2+} varied substantially among freshwater inputs to the three study sites (Figure 2). Roskilde Fjord had the highest levels and Ringkøbing Fjord had the lowest levels for all three constituents. pH varied seasonally with peaks around April–May in all three catchments (Figure 2a), whereas A_T displayed weak seasonal patterns (Figure 2c) with the highest and lowest values in summer and winter, respectively, for Ringkøbing Fjord (range: 0.61–0.83 mmol kg^{-1}) and Skive Fjord (range: 1.59–1.88 mmol kg^{-1}). Due to the lower number of A_T observations in Roskilde Fjord, no distinctive seasonal pattern could be discerned. Ca^{2+} concentrations in Ringkøbing Fjord did not exhibit any distinctive seasonal pattern, but in Roskilde Fjord and Skive Fjord opposing seasonal patterns were observed (Figure 2e). Freshwater Ca^{2+} concentrations were highest in Roskilde Fjord during winter and in Skive Fjord during summer, and lowest in Roskilde Fjord during summer and in Skive Fjord during winter.

The earliest pH data date back to 1973 in Roskilde Fjord streams, but up to the mid-1980s observations were few in the Roskilde Fjord and Skive Fjord catchments, resulting in considerable uncertainty of the annual means (Figure 2b). In these two systems, pH did not change substantially over time with annual means fluctuating around 7.9 and 7.6 in Roskilde Fjord and Skive Fjord, respectively (Table 2). On the other hand, pH in freshwater input to Ringkøbing Fjord increased steadily from around 6.9 to 7.2 over four decades of monitoring. A_T in the freshwater input to Ringkøbing Fjord and Roskilde Fjord remained relatively constant over time at levels of 0.73 mmol kg^{-1} and 5.2 mmol kg^{-1}, respectively, whereas A_T in the freshwater input to Skive Fjord increased from around 1.5 mmol kg^{-1} in the early 1980s to almost 2.0 mmol kg^{-1} in recent years (Figure 2d). The increasing trend in Skive Fjord was included for calculating the freshwater end-member A_T. Ca^{2+} concentrations did not exhibit any major change over the few years with monitoring data, yielding levels of 0.68, 3.00, and 1.57 mmol kg^{-1} for Ringkøbing Fjord, Roskilde Fjord, and Skive Fjord, respectively (Figure 2f).

The three outer boundary stations were not monitored as frequently and for as long as the stations within the coastal systems and in the streams. Seasonal variations in pH typically ranged by approximately 0.3 at all three boundary stations with the lowest levels in winter and highest in summer (Figure S2). Ringkøbing Fjord boundary station did not exhibit any seasonal variation in A_T, whereas A_T the two other boundary stations varied seasonally, largely paralleling seasonal variations in salinity. None of the three boundary stations displayed any particular trend in the interannual values. The three boundary stations had similar mean levels for pH (7.92–7.93), whereas mean A_T levels ranged from 1.97 mmol kg^{-1} for Roskilde Fjord,
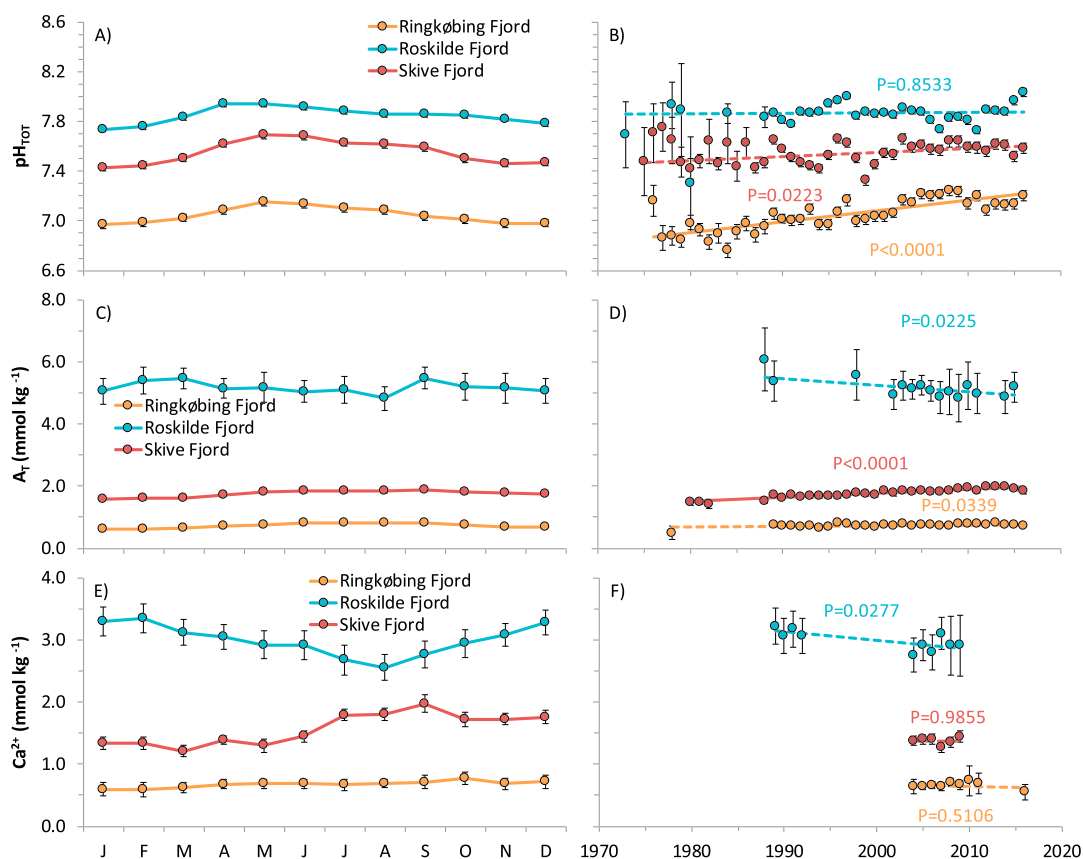
Figure 2. Monthly and annual means of (a, b) pH, (c, d) total alkalinity (A_T), and (e, f) dissolved calcium (Ca^{2+}) concentrations in the freshwater input to the three studied coastal systems. The means were derived as marginal means of the month and year factors in equation (1). Error bars mark the 95% confidence interval of means. Linear trends in the annual means are shown in the right-hand panel with solid lines for $P < 0.01$ and dashed lines for $P > 0.01$.

Table 2
Trend Analyses for Variables in the Carbonate System for Freshwater, Outer Boundary and Estuarine Conditions, Adjusted for Salinity- and Temperature-Dependent Effects on the Carbonate System Constants (CS) and Mixing (MX)

Variable	Ringkøbing Fjord		Roskilde Fjord	Skive Fjord
Freshwater input	1977–2016		1973–2016	1975–2016
A_T	0.0021 ($P = 0.0339$)		−0.0207 ($P = 0.0225$)	**0.0128 ($P = 0.0001$)**
pH_{TOT}	**0.0088 ($P < 0.0001$)**		0.0003 ($P = 0.8533$)	0.0032 ($P = 0.0223$)
DIC	−0.0000 ($P = 0.9951$)		−0.0221 ($P = 0.0369$)	**0.0075 ($P < 0.0001$)**
Outer boundary	1989–1997		1993–2003	1982–1997
A_T	0.0032 ($P = 0.4832$)		0.0039 ($P = 0.7587$)	0.0197 ($P = 0.2135$)
pH_{TOT}	0.0119 ($P = 0.4399$)		−0.0109 ($P = 0.0461$)	−0.0023 ($P = 0.6159$)
DIC	−0.0004 ($P = 0.9311$)		−0.0026 ($P = 0.8816$)	0.0190 ($P = 0.2051$)
Estuary	1980–1995	1996–2016	1972–2016	1980–2010
A_T	**0.0226 ($P = 0.0003$)**	−0.0031 ($P = 0.4890$)	**0.0190 ($P = 0.0032$)**	**0.0188 ($P = 0.0002$)**
A_T (adj. MX)	0.0123 ($P = 0.0113$)	0.0008 ($P = 0.8357$)	0.0030 ($P = 0.6360$)	0.0123 ($P = 0.0147$)
pH_{TOT}	**0.0214 ($P < 0.0001$)**	**−0.0088 ($P < 0.0001$)**	**−0.0031 ($P = 0.0080$)**	**−0.0061 ($P = 0.0011$)**
pH_{TOT} (adj. CS)	**0.0259 ($P < 0.0001$)**	**−0.0100 ($P < 0.0001$)**	**−0.0036 ($P = 0.0034$)**	−0.0040 ($P = 0.0317$)
pH_{TOT} (adj. MX)	**0.0167 ($P = 0.0002$)**	**−0.0103 ($P = 0.0017$)**	−0.0027 ($P = 0.1047$)	**−0.0062 ($P = 0.0058$)**
DIC	**0.0151 ($P = 0.0040$)**	−0.0060 ($P = 0.0607$)	0.0075 ($P = 0.0292$)	**0.0062 ($P < 0.0001$)**
DIC (adj. MX)	0.0077 (0.0788)	−0.0014 ($P = 0.6480$)	0.0033 ($P = 0.1233$)	**0.0034 ($P = 0.0017$)**
pCO_2	**−33.8 ($P = 0.0014$)**	**12.4 ($P < 0.0001$)**	**7.81 ($P < 0.0001$)**	**8.06 ($P = 0.0009$)**
pCO_2 (adj. CS)	**−46.3 ($P = 0.0002$)**	**13.5 ($P < 0.0001$)**	**7.05 ($P = 0.0005$)**	**6.46 ($P = 0.0075$)**
pCO_2 (adj. MX)	0.331 ($P = 0.9747$)	**31.9 ($P < 0.0001$)**	−3.14 ($P = 0.6622$)	6.01 ($P = 0.1081$)

Note. The rates of change are in mmol kg^{-1} yr^{-1} for A_T and dissolved inorganic carbon (DIC), in pH units yr^{-1}, and µatm yr^{-1} for pCO_2. Significant trends ($P < 0.01$) are highlighted in bold. Note that trend periods are shorter for A_T in Roskilde Fjord and Skive Fjord, where A_T was not measured in all years.
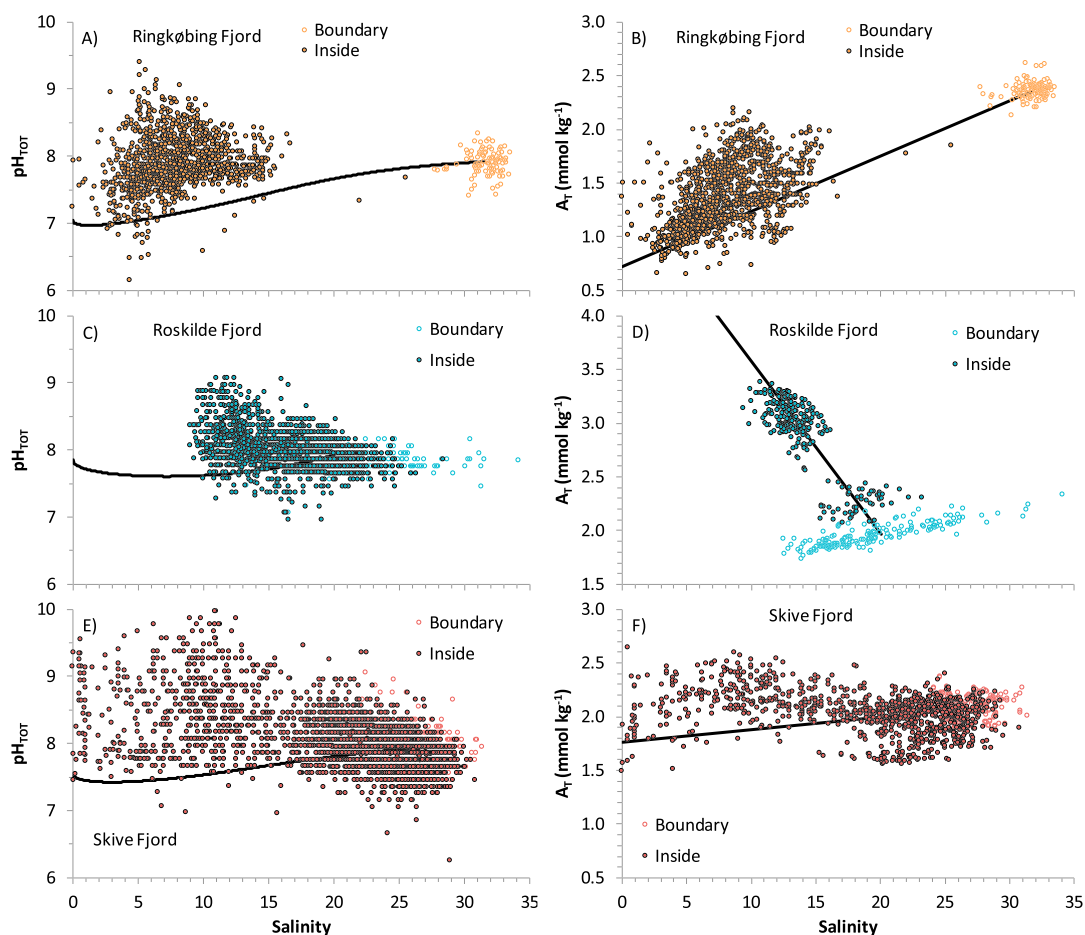
Figure 3. Measured (a, c, e) pH and (b, d, f) A_T across salinity gradients in the three estuaries and boundary stations. Solid lines indicate conservative mixing between mean pH and A_T at the freshwater and outer boundary end-members. Mixing lines for pH were calculated from conservative mixing of end-member means of A_T and dissolved inorganic carbon, the latter calculated from end-member means of A_T and pH.

2.07 mmol kg^{-1} for Skive Fjord, to 2.35 mmol kg^{-1} for Ringkøbing Fjord. Surprisingly, this ranking of A_T levels at the boundary stations was inverse to the levels in the freshwater input, yielding contrasting A_T gradients with salinity in the three estuaries.

4.2. Gradients From Fresh to Open Waters

Freshwater mean pH was slightly lower than the marine end-member, most pronounced for Ringkøbing Fjord (Figure 3). However, pH measurements within the coastal systems were generally higher than at the two end-members, peaking at intermediate salinities (typically between 5 and 10) with pH levels up to 2.5 units higher than predicted by conservative mixing. Even at low salinities (between 0 and 5) elevated pH levels were observed, whereas pH observations gradually approached the mixing line for salinities above 10. Variability in pH spanned up to 3 units for a given salinity.

The three coastal systems displayed different A_T variations across salinity gradients; increasing in Ringkøbing Fjord, decreasing in Roskilde Fjord, and almost no change in Skive Fjord (Figure 3). Overall, A_T observations generally followed the mixing line between the two end-members, although with considerable variation (up to 1 mmol kg^{-1}) around the line. Variations in both salinity and A_T were relatively small at the boundary stations for Ringkøbing Fjord and Skive Fjord, whereas the boundary station for Roskilde Fjord displayed large variations in both salinity and A_T with a relationship governed by mixing of Baltic Sea and Skagerrak waters. A_T displayed a tendency with slightly higher values than the conservative mixing line in Ringkøbing Fjord (Figure 3b). A_T in the inner and outer part of Roskilde Fjord constituted two separate clusters with different mixing relationships to salinity (Figure 3d). A_T in the inner part of Roskilde Fjord
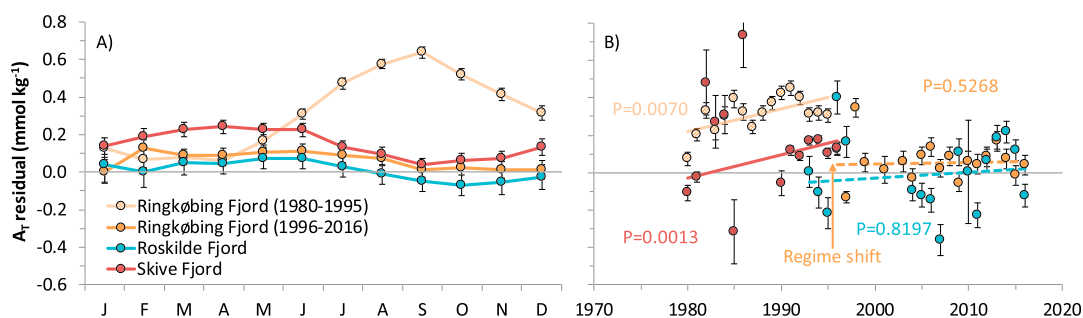
Figure 4. (a) Monthly and (b) annual variations in A_T residuals from conservative mixing between fresh and marine end-members (equation (3)). The means were derived as marginal means of the month and year factors in equation (4). Error bars mark the 95% confidence interval of means. Linear trends in the annual means are shown in Figure 4b with solid lines for $P < 0.01$ and dashed lines for $P > 0.01$. The timing of the regime shift in Ringkøbing Fjord is indicated with an arrow.

generally followed the mixing line between the two end-members, whereas the salinity-A_T relationship for the outer part more resembled that of the boundary station. In Skive Fjord, A_T exhibited departures from pure mixing along the salinity gradient with generally higher levels around 10 and lower levels around 20 (Figure 3f).

In fact, A_T showed systematic departures from conservative mixing when analyzing the residuals (Figure 4a). Prior to the regime shift Ringkøbing Fjord was a substantial source of A_t in May–September (increasing deviations from conservative mixing) and a sink from October to February (decreasing deviations). After the regime shift departures from conservative mixing were substantially smaller and resembled the seasonal pattern of the two other estuaries, that is, a source of A_T during winter and a sink during summer with ranges of 0.1–0.2 mmol kg^{-1}. The residuals from conservative mixing increased over time up to the regime shift in Ringkøbing Fjord, whereas no changes were observed after the regime shift, as was also the case for Roskilde Fjord (Figure 4b). In Skive Fjord, the A_T residuals increased from 1980 to 1996 but this trend was mainly driven by the first 2 years.

4.3. Experienced Trends

Seasonal pH variations were considerable, typically ranging ~0.4 unit from the lowest values in December–February to the highest in April–June, and even 1 unit during the productive years before the regime shift in Ringkøbing Fjord (Figure 5a). pH decreased over time in Roskilde Fjord and Skive Fjord by 0.0031 and 0.0061 year^{-1} (Figure 5b and Table 2), respectively, during a period when both estuaries experienced a temperature increase by 0.05°C yr^{-1} and no specific trend in salinity (Figure S3). Ringkøbing Fjord, on the other hand, exhibited quite different pH trends before and after the regime shifts with an increase of 0.021 year^{-1} before the regime shift and a decrease by 0.009 year^{-1} after the regime shift (Table 2). In both periods the temperature increase in Ringkøbing Fjord was similar to the two other estuaries (0.5°C per decade), but salinity increased before the regime shift and decreased after the regime shift (Figure S3).

DIC in Ringkøbing Fjord varied strongly before the regime shift from 1.11 mmol kg^{-1} in April to 1.74 mmol kg^{-1} in September (Figure 5c), but this strong seasonal variation was dampened after the regime shift (range of 0.34 mmol kg^{-1}). DIC seasonal variations were smaller in Roskilde Fjord and Skive Fjord (ranges of 0.12 and 0.28 mmol kg^{-1}, respectively), with the lowest levels in February for Roskilde Fjord and in September for Skive Fjord. DIC annual means generally increased in Skive Fjord and Ringkøbing Fjord before the regime shift, whereas levels did not change significantly in Roskilde Fjord and Ringkøbing Fjord after the regime shift (Figure 5d).

DIC trends were partly mirrored in pCO$_2$ trends for Roskilde Fjord and Skive Fjord, but for Ringkøbing Fjord trends in pCO$_2$ were opposing those of DIC (Figure 5f). In both Roskilde Fjord and Skive Fjord pCO$_2$ increased significantly by ~8 μatm yr^{-1}, whereas pCO$_2$ levels in Ringkøbing Fjord first declined by 34 μatm yr^{-1} and then increased by 12 μatm yr^{-1}. The more saline Skive Fjord had the lowest levels of pCO$_2$, whereas pCO$_2$ levels in Roskilde Fjord and Ringkøbing Fjord were more comparable despite large difference in pH and DIC (Figures 5b and 5d). All three estuaries displayed similar seasonal patterns with high pCO$_2$ in winter months and low levels during summer (Figure 5e). The largest seasonal variation was seen in Ringkøbing
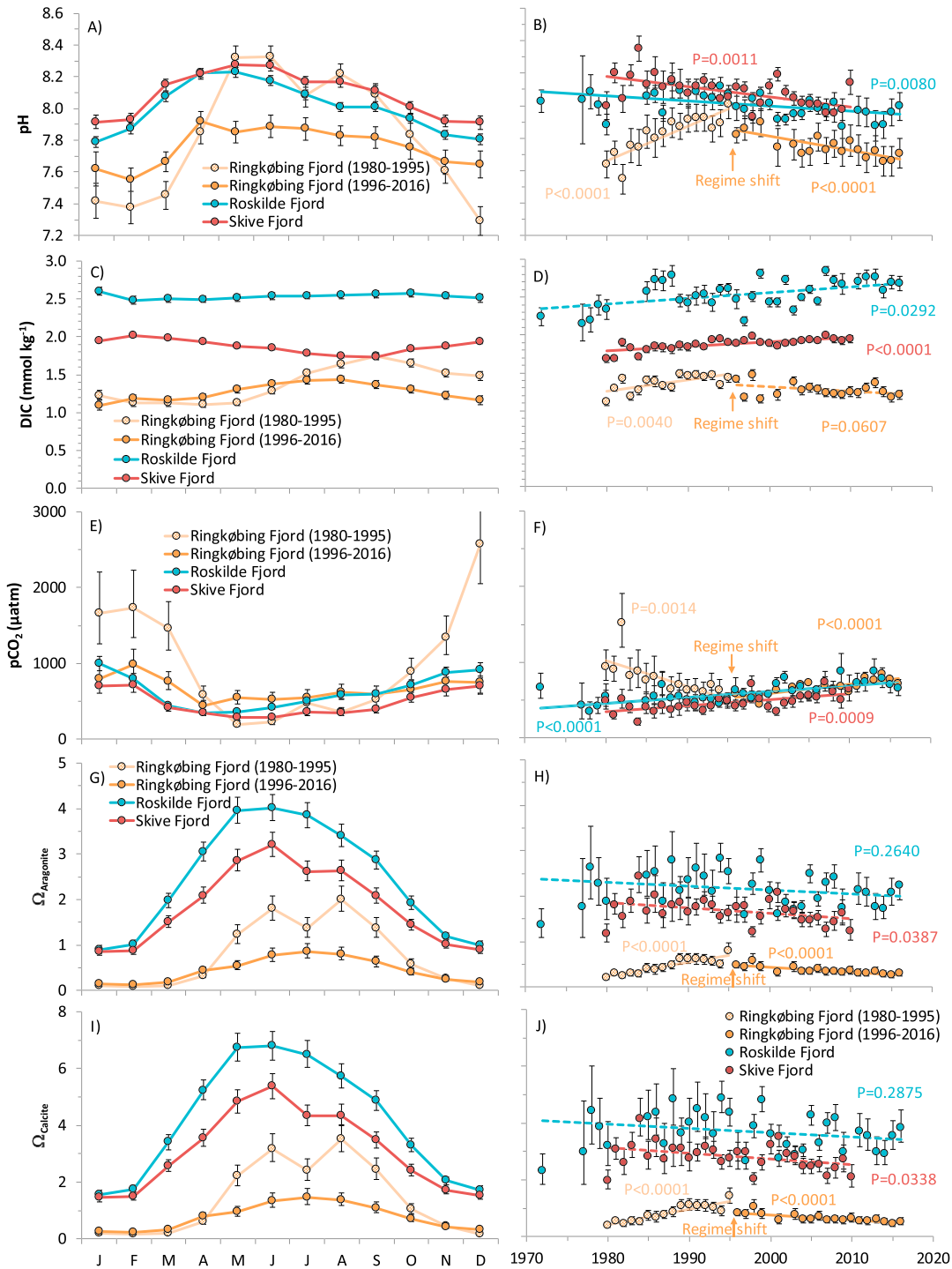
Figure 5. (left) Monthly and (right) annual means of (a, b) pH, (c, d) DIC, (e, f) pCO$_2$, and (g–j) calcium carbonate saturation states in the three studied coastal systems. The means were derived as marginal means of the month and year factors in equation (2). Error bars mark the 95% confidence interval of means. Linear trends in the annual means are shown in the right-hand panels with solid lines for $P < 0.01$ and dashed lines for $P > 0.01$. The timing of the regime shift in Ringkøbing Fjord is indicated with an arrow.

Fjord before the regime shift, ranging from almost 2,600 μatm in December to 200 μatm in May. Levels of pCO$_2$ were only below atmospheric equilibrium for May, June, and August in Ringkøbing Fjord before the regime shift, April and May in Roskilde Fjord, and April–September in Skive Fjord. In all other months, CO$_2$ was supersaturated relative to the atmospheric CO$_2$ level, resulting in CO$_2$ outgassing.
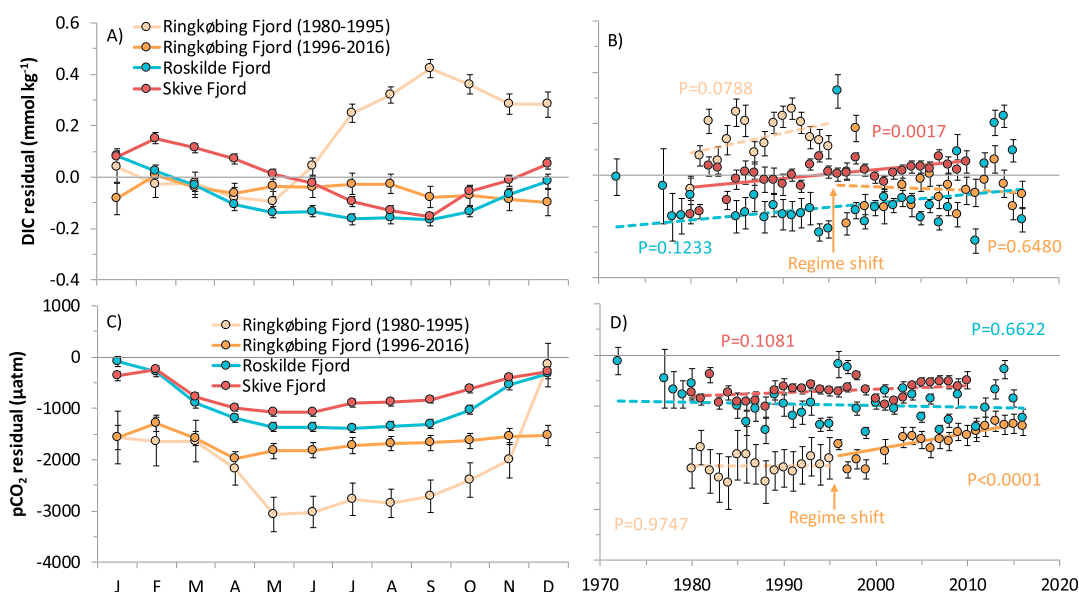
Figure 6. Monthly and interannual variations in residuals from conservative mixing (equation (3)) for calculated (a, b) dissolved inorganic carbon (DIC) and (c, d) pCO_2 in the three studied coastal systems. The means were derived as marginal means of the month and year factors in equation (4). Error bars mark the 95% confidence interval of means. Linear trends in the annual means are shown in the right-hand panels with solid lines for $P < 0.01$ and dashed lines for $P > 0.01$. The timing of the regime shift in Ringkøbing Fjord is indicated with an arrow.

Saturation states for aragonite and calcite had similar temporal variations across the three estuaries (Figures 5g–5j). Saturation states were highest in Roskilde Fjord, followed by Skive Fjord and Ringkøbing Fjord. In Roskilde Fjord and Skive Fjord, $\Omega_{Aragonite}$ and $\Omega_{Calcite}$ were close to or above 1 throughout most of the year, but in Ringkøbing Fjord aragonite and calcite saturation was only experienced in summer months—primarily before the regime shift. Significant trends in $\Omega_{Aragonite}$ and $\Omega_{Calcite}$ were observed for Ringkøbing Fjord only, increasing before the regime shift followed by a decrease.

4.4. Trends Adjusted for Mixing, Salinity, and Temperature Effects

The effect of salinity and temperature on carbonate system constants was assessed by comparing pH and pCO_2 trends with those from standardized values. Recalculating pH and pCO_2 for standard salinity of 15 and temperature of 10°C emphasized seasonal patterns; increasing typical pH ranges by ~0.1 additional unit (i.e., typical range of 0.5 unit) and increasing/decreasing pCO_2 levels during winter/summer (data not shown). The overall long-term trends for these standardized variables were similar to experienced trends (Figures 5b and 5f), although pCO_2 changes over time were slightly smaller in Roskilde Fjord and Skive Fjord (7.1 and 6.3 μatm yr^{-1}, respectively) and slightly larger in Ringkøbing Fjord (-46.3 μatm yr^{-1} before and 13.5 μatm yr^{-1} after the regime shift). Interestingly, pH trends in Roskilde Fjord and Skive Fjord were more similar (-0.0036 year^{-1} and -0.0040 year^{-1}, respectively) when adjusted to standard salinity and temperature.

Residual variation, after accounting for mixing as well as temperature and salinity effects on carbonate system constants, described the effect of biological processes and changing atmospheric pCO_2. Accounting for mixing between freshwater and marine end-members had a larger effect on the seasonal scale as well as long-term trends in Ringkøbing Fjord, where changes in salinity were considerable (Figure S3). In Ringkøbing Fjord, DIC seasonal variations correlated with salinity because DIC increased toward the marine end-member, and adjusting for estuarine mixing reduced the DIC seasonal range from 0.64 mmol kg^{-1} (Figure 5c) to 0.52 mmol kg^{-1} (Figure 6a) before the regime shift, and similarly from 0.34 to 0.11 mmol kg^{-1} after the regime shift. Thus, a substantial part of the DIC seasonal variation in Ringkøbing Fjord could be explained by mixing. However, in Roskilde Fjord and Skive Fjord observed seasonal patterns were dampened by salinity variations and accounting for mixing actually increased seasonal ranges by 0.13 and 0.02 mmol kg^{-1}, respectively. In both of these estuaries, there was a net DIC removal during spring and summer, changing to a net DIC supply during autumn (Figure 6a). There was a large DIC supply to Ringkøbing Fjord in summer before the regime shift (ΔDIC = 0.52 mmol kg^{-1}), whereas DIC was removed

from the system in other parts of the year. DIC changes over time were significant only for Skive Fjord, increasing by 0.003 mmol kg^{-1} yr^{-1}, although trends of similar magnitude were observed also for Roskilde Fjord and Ringkøbing Fjord before the regime shift (Figure 6b).

Estuarine levels of pCO$_2$ were consistently lower than predicted by conservative mixing of the two end-members (Figure 6c). CO$_2$ was removed during spring and supplied during autumn in Roskilde Fjord, Skive Fjord, and Ringkøbing Fjord before the regime shift, whereas after the regime shift pCO$_2$ was removed only in March and April and supplied throughout the rest of the year. Only Ringkøbing Fjord experienced significantly increasing CO$_2$ levels from 1996 to 2016 (Figure 6d) when accounting for mixing and salinity and temperature effects on carbonate system constants.

5. Discussion

Carbonate chemistry in coastal waters is governed by a range of physical and biogeochemical processes, which may have opposite effects on pH, A_T, pCO$_2$, and DIC levels. Changes in salinity and temperature affect solubility and speciation of the carbonate system, and consequently, levels of pH and pCO$_2$. Coastal ecosystems and estuaries, in particular, are characterized by intense mixing of water masses with different physicochemical properties, causing large variations in the carbonate system. Particularly, upwelling and intrusions of oxygen-depleted and CO$_2$-rich waters drastically alter pH, pCO$_2$, and DIC levels (Feely et al., 2008; Melzner et al., 2013). Precipitation and evaporation further dilute and concentrate substances, including salinity with secondary effects on solubility and dissociation. Moreover, atmospheric deposition of sulfur and nitrogen compounds affects the coastal carbonate chemistry, which is also changed by different biogeochemical processes (calcification/decalcification, nitrification, denitrification, primary production, nutrient assimilation and remineralization, and formation of pyrite, vivianite, and other nutrient mineral forms) to a varying degree (Reed et al., 2016; Wolf-Gladrow et al., 2007). The large seasonal variability (Figures 4–6) indicates dominance of biogeochemical processes for regulating coastal carbonate systems.

Long-term changes in coastal pH (Duarte et al., 2013; Provoost et al., 2010; Waldbusser et al., 2011) and A_T (Hu et al., 2015) have been described along with possible explanations for the observed trends. Our study confirms that coastal acidification deviates substantially from ocean acidification and that A_T export from land may have increased (Duarte et al., 2013). However, our study is the first to disentangle the effects of physical and biogeochemical processes on long-term changes in coastal carbonate chemistry.

5.1. Effects of Salinity, Temperature, and Mixing

Carbonate chemistry shifted toward more carbonic acid with increasing temperature and salinity, which will affect pH and pCO$_2$ variations on seasonal and long-term scales. Due to the nonlinear nature of the carbonate system, pCO$_2$ levels will approximately double relative to increases in DIC and this effect will be amplified with increasing temperature and salinity (Melzner et al., 2013). Trends in pCO$_2$ (Figure 5f) were also more pronounced than DIC trends (Figure 5d) due to the nonlinearity of the carbonate system with levels changing by factor of 2 over time. Increasing pCO$_2$ could partly be explained by temperature increase (Figure S3) in Roskilde Fjord and Skive Fjord, where trends were moderated by temperature and salinity standardization (10–20% reduction of trend; Table 2). On the other hand, the effect of changing salinity and temperature on DIC speciation and CO$_2$ solubility amplified the pCO$_2$ trends in Ringkøbing Fjord. Nevertheless, increasing temperature and CO$_2$ in the atmosphere will synergistically increase marine pCO$_2$ levels in the future.

A_T and pH in shallow coastal systems located in arid or semiarid areas are affected by changes in the precipitation/evaporation balance (Hu et al., 2015). Although A_T increases with evaporation, reduced A_T inputs during drought conditions are generally more important for regulating pH and A_T levels in coastal ecosystems (Cai et al., 2008; Hu et al., 2015). The average precipitation in Denmark is ~700 mm yr^{-1} with an almost even distribution among seasons, which is approximately balanced by surface evaporation during summer. In winter, evaporation is negligible due to low temperatures and high relative humidity, and hence, there is a net dilution effect from rain, but this effect is small compared to the freshwater input, as the catchment areas are about 10 times larger than the estuarine surface areas (Table 1). Thus, seasonal and interannual variations in the precipitation/evaporation balance are relatively unimportant for the three studies estuaries. However, in other types of catchments with granite or limestone changing precipitation can effect freshwater inputs of pH and A_T (Hjalmarsson et al., 2008).

Atmospheric depositions of SO_x, NO_x, and NH_x peaked in the 1980s and have gradually declined. The long-term influence on pH in Kattegat surface waters have been estimated to be of ~0.001 per decade (Omstedt et al., 2015), and thus of marginal importance compared to other processes.

Different pH and A_T levels at the freshwater and marine end-members, most pronounced for Ringkøbing Fjord and Roskilde Fjord (Figure 3), lead to large variability in the coastal carbonate system due to mixing. This large variability has been demonstrated in the Scheldt Estuary (Borges & Abril, 2011; Frankignoulle et al., 1998), the Mekong delta (Borges & Abril, 2011), and the Baltic Sea (Beldowski et al., 2010), but none of these studies attempted to partition the variability into physical mixing and biogeochemical processes. Salinity varied seasonally in all three study sites and Ringkøbing Fjord experienced changes in annual means from ~5 to ~10 (Figure S3). From the conservative mixing relationships (Figure 3) we estimate that the range of seasonal variation in salinity (Figure S3) can account for seasonal changes in pH of 0.008 in Roskilde Fjord, 0.034 in Skive Fjord, and 0.116 and 0.186 in Ringkøbing Fjord before and after the regime shift. However, observed pH seasonality was substantially larger and somewhat out of phase with salinity (Figure 5a). Similarly, seasonal variation in salinity can account for seasonal changes in A_T of 0.028 mmol kg^{-1} in Skive Fjord, 0.31 mmol kg^{-1} in Roskilde Fjord, and 0.21 and 0.35 mmol kg^{-1} in Ringkøbing Fjord before and after the regime shift. Although mixing is important for describing variations in A_T, systematic variations remained (Figure 4) that were associated with biogeochemical processes.

5.2. Total Alkalinity in Estuarine Environments

A_T is often used as a conservative tracer at ocean margins influenced by large rivers (Cai et al., 2010; Fransson et al., 2001). However, recent studies have suggested that consumption/production of A_T within shallow estuaries can be important (Hu et al., 2015; Waldbusser et al., 2013). Carbonate-producing organisms consume A_T, and A_T deficiency with respect to conservative mixing has been attributed to calcification through shell aggregation of bivalves. However, other processes such as nitrification, denitrification, uptake, and release of ammonia and nitrate also contribute as A_T sources and sinks (Wolf-Gladrow et al., 2007). We observed winter A_T production and summer A_T consumption in Roskilde Fjord, Skive Fjord, and Ringkøbing Fjord after the regime shift; a pattern consistent with a relatively constant rate of decalcification from shell dissolution and calcification intensifying with temperature over summer. Benthic communities are dominated by dense populations of bivalves in all three coastal ecosystems (except Ringkøbing Fjord prior to the regime shift) and since all three systems have relatively long residence times (Table 1), it is likely that bivalve calcification/decalcification affected A_T cycling. A_T uptake from June to September ranged between 0.10 and 0.17 mmol kg^{-1}, which combined with the average depths translates into a shell aggregation of 10–45 g $CaCO_3$ m^{-2} (using $\Delta CaCO_3 = -2 \times \Delta A_T$ on the molar scale). For comparison, Petersen et al. (2008) reported mollusk biomass of 100–200 g DW m^{-2} in Ringkøbing Fjord after the regime shift, and Josefson and Rasmussen (2000) reported values in the same range for 14 other Danish estuaries. Therefore, it is likely that bivalves in shallow coastal systems with long residence times can modify A_T seasonally by ~0.1–0.2 mmol kg^{-1}.

Temporal changes in A_T in Ringkøbing Fjord before the regime shift were more complicated (Figure 4). A_T production increased by 0.58 mmol kg^{-1} from April to September, and this A_T increase was consumed again by February (Figure 4a). This seasonal pattern indicates a strong mismatch between processes producing and consuming A_T, and this decoupling appeared to increase with time up to the regime shift in 1996 (Figure 4b).

In this period the biomass of the benthic fauna was low and dominated by polychaetes (Petersen et al., 2008), implying that calcification was negligible. On the other hand, decalcification of shell deposits could be a potential A_T source. Ringkøbing Fjord has experienced higher salinity regimes in the past and it is likely that the lagoon was inhabited by dense colonies of bivalves during such regimes. However, salinity remained low from construction of the sluice gate in 1931 until the regime shift in 1996, that is, a period of 65 years largely without calcifiers. Shell dissolution typically operates on a decadal scale with a half-life for oyster and mussel shells between 3 and 10 years (see Waldbusser et al., 2013, and references therein). Given the long low-salinity period prior to our study period, we argue that A_T inputs from shell dissolution were negligible.

Due to the overall low grazing pressure, there was a large accumulation of algae biomass, particularly during summer. Although concentrations of different nitrogen species do not contribute to A_T in general, A_T

increases from nitrate assimilation by algae ($\Delta A_T = -\Delta NO_3^-$) due to the electroneutrality of the cell (Wolf-Gladrow et al., 2007). Nitrogen inputs from land are mostly in the form of nitrate, and freshwater concentrations before the regime shift were typically 200–400 μmol L^{-1} with corresponding winter nitrate maximum values of ~200 μmol L^{-1} (data not shown). Thus, it is possible that the accumulation of algae biomass fueled by high nitrate inputs could cause a seasonal imbalance between A_T production and consumption, and partly explain the large seasonal variation in A_T. There was no accumulation of ammonia throughout the year (data not shown), suggesting that ammonia release and subsequent nitrification ($\Delta A_T = -1$ in combination) could be dominant during autumn and winter. Thus, large accumulation of phytoplankton biomass due to low grazing can create a seasonal shift in A_T. However, the accumulation of A_T from April to September (ΔA_T = 0.58 mmol kg^{-1}) was paralleled by an almost similar increase in DIC from May to September (ΔDIC = 0.52 mmol kg^{-1}). Although the DIC increase could also be explained by sediment respiration, this concomitant increase in A_T and DIC points toward sulfate reduction (Cai et al., 2017).

Even though oxygen depletion occurred only occasionally in this usually well-mixed lagoon even before the regime shift, it is possible that the observed residual A_T increase from April to September (Figure 4a) was influenced by anaerobic degradation processes in the sediments (e.g., denitrification and sulfate reduction). Sediments can be anoxic/sulfidic just a few centimeters or millimeters below the sediment surface even when the overlying water is oxic, particularly in the absence of macrobenthic bioturbators. The observed seasonal pattern was also consistent with that expected for sulfate reduction and redoxcline movement in the sediments (Jørgensen & Sørensen, 1985). The gradual residual A_T decline observed in autumn and winter could similarly have been influenced by oxidation of, for example, ammonium and sulfide accumulated in pore water.

Using the basin characteristics (Table 1), the A_T increase in Ringkøbing Fjord from April to September corresponds to an average areal flux of approximately 7.5 mmol m^{-2} d^{-1}. In fact, measurements by Brenner et al. (2016) at numerous sites in the Southern North Sea revealed sediment to water A_T fluxes in a range 0–21-.4 mmol m^{-2} d^{-1} (mean: 6.6 mmol m^{-2} d^{-1}). In a numerical experiment, including A_T sources and sinks in both sediments and water column, Brenner et al. (2016) calculated a net A_T generation in the water column of 2.4 mmol m^{-2} d^{-1}. They identified the main A_T sources as pelagic primary production and benthic CaCO$_3$ dissolution, denitrification, and sulfate reduction. The main A_T sinks were identified as aerobic respiration and CaCO$_3$ formation in the water column, and further nitrification and sulfide oxidation in the sediments.

On annual basis, the A_T residual in Ringkøbing Fjord before the regime shift was approximately 0.3–0.4 mmol kg^{-1} yr^{-1} (Figure 4b) corresponding to an average net areal flux of 1.6–2.1 mmol m^{-2} d^{-1}, similar to the estimate by Brenner et al. (2016) for the Southern North Sea. The conspicuous seasonal A_T development in Ringkøbing Fjord thus appears to support substantial internal A_T fluxes mediated by biogeochemical processes. After the regime shift this A_T source largely (but not completely) disappeared, and the increasing pH trend coupled to the large net A_T generation before the regime shift instead turned into a declining trend (Figure 5b).

5.3. Acidification Effects From Oligotrophication

Increasing CO$_2$ in the atmosphere yields pH declines in the oceans at rates of 0.002 year^{-1} (Doney, 2010; Olafsson et al., 2009), but pH declines have been even stronger on continental shelves (Reimer et al., 2017) and in coastal areas where nutrient inputs have been reduced (e.g., Duarte et al., 2013). The large monthly variation in pH and pCO$_2$ (with and without adjusting for mixing) highlights the importance of metabolic processes in the three studied systems on the seasonal scale. On the long-term scale, we observed pH declines that were 2–4 times higher than ocean acidification (0.0031–0.0088 year^{-1}) but also increases in Ringkøbing Fjord during the productive period before the regime shift (0.0214 year^{-1}). Although the large trends in Ringkøbing Fjord were partly due to changing salinity, pH trends in Roskilde Fjord and Skive Fjord (no trend in salinity, Figure S3) were still considerably stronger than the ocean acidification trend. In these two systems, long-term pH trends, adjusted for salinity and temperature effects on DIC speciation, were about twice that of ocean acidification. Further, for each 1°C increase in temperature the pH decrease is ~0.015 based solely on effects of dissociation and dissolution. With a temperature increase of 0.05°C yr^{-1}, pH has decreased by 0.0008 year^{-1} (about half the rate of ocean acidification) from this effect alone. Thus, in the studied coastal

systems pH has declined from oligotrophication and increased CO_2 in the atmosphere as well as warming by a rate approximately 2.5 times that of the ocean.

Indeed, pCO_2 trends in Roskilde Fjord and Skive Fjord (Figure 5f) were 4 times higher than oceanic pCO_2 trends (1.88 μatm yr^{-1}; Doney, 2010), and even when adjusting for mixing, DIC speciation and CO_2 solubility, pCO_2 trends were still 2–3 times higher (Table 2). Hence, these two systems have been enriched with CO_2 over time, indicating a lower phytoplankton uptake, which is also consistent with increasing DIC concentrations. The negative pCO_2 residuals (Figure 6d) indicate a net CO_2 uptake in all three systems, with considerably larger uptake in Ringkøbing Fjord before the regime shift, approaching that of the two other systems in recent years. However, there was no trend in the pCO_2 residuals before the regime shift (Table 2), suggesting that the experienced decline in pCO_2 before the regime shift in Ringkøbing Fjord (Figure 5f) was mainly caused by larger exchange with the open boundary and increasing salinity. Consequently, hydrological control of coastal ecosystems can alter the carbonate chemistry even more drastically than changing atmospheric CO_2, nutrient inputs and temperature.

Inputs of organic matter and nutrients from land regulate the balance between production and respiration in coastal systems (Borges & Gypens, 2010). Improved sewage treatment has reduced inputs of both organic matter and nutrients to coastal systems, altering the biogeochemistry of coastal systems with dominant input from point sources (Soetart et al., 2006). In recent decades, nutrient reductions from diffuse sources have also been successfully achieved, primarily in North America and northwestern Europe (Carstensen et al., 2006; Nixon, 2009). Coastal systems dominated by agriculture land use receive freshwater inputs rich in inorganic nutrients (Riemann et al., 2016). Although nutrient management plans were implemented to reduce the adverse effects of eutrophication, our results document associated declines in pH. Thus, we submit that abating eutrophication, a severe problem for many coastal ecosystems, may also unexpectedly enhance coastal acidification with pH declining at rates much larger than ocean acidification.

5.4. Potential Biological Effects

Experiments have revealed that calcifying marine organisms are expected to be particularly susceptible to future pH changes (Dupont & Pörtner, 2013), although the consequences on ecosystem scale are generally not understood in detail (Doney et al., 2009; Havenhand, 2012). For example, the coccolithophore *Emiliania huxleyi* is already in a competitive disadvantage in the Baltic Sea because calcite and aragonite are undersaturated in winter (Tyrrell et al., 2008), but the potential consequences for the phytoplankton community and biogeochemical cycles have not been addressed. $CaCO_3$ does not readily dissolve for Ω values above 1, implying that current Ω levels in Roskilde Fjord and Skive Fjord (Figure 5g) are not affecting calcifiers. Aragonite saturation states <1 in Ringkøbing Fjord could potentially limit calcification and pose a threat to calcifiers, but such conditions prevail mainly in winter months (Figure 5) when calcification is low, and since marine organisms can prevent external dissolution at $\Omega < 1$ (Ries et al., 2009; Thomsen et al., 2010), calcifiers are not believed to be affected by current Ω levels in Ringkøbing Fjord. In fact, the massive colonization by *Mya arenaria* after the regime shift in Ringkøbing Fjord (Petersen et al., 2008) occurred despite Ω values around 1 in summer months. Hence, this finding supports that calcification takes place even at $\Omega < 1$ even if it is a more energy-demanding process at low Ω (Dupont et al., 2010; Liescka & Riebesell, 2012; Ries et al., 2009; Thomsen et al., 2010). Nevertheless, continued coastal acidification will increase the dissolution potential in the future.

High levels of pCO_2 stimulate production of organic matter (Spilling et al., 2016), but it also has repercussions on the acid-base regulation of marine organisms. Heterotrophic metazoans maintain respiratory diffusion gradients through increased pCO_2 in their body fluid, which can have physiological consequences such as internal shell dissolution, oxidative stress and increased energetic costs (Melzner et al., 2013). Typical values of extracellular pCO_2 range from 1,000 to 4,000 μatm (Melzner et al., 2009), which is generally higher than observed pCO_2 (Figure 5e). In unicellular organisms, pCO_2 equals that of the environment, and hence, these organisms will be exposed to larger fluctuations in intracellular pCO_2 but consequences thereof are poorly assessed. However, due to the short generation times of these organisms, it is possible that they can genetically adapt to increasing pCO_2 as opposed to long-lived metazoans (Melzner et al., 2009). Moreover, high levels of pCO_2 can exacerbate physiological effects of hypoxia (Brewer & Peltzer, 2009), but biological effects of this cocktail remain understudied (Melzner et al., 2013).

References

Beldowski, J., Löffler, A., Schneider, B., & Joensuu, L. (2010). Distribution and biogeochemical control of total CO_2 and total alkalinity in the Baltic Sea. *Journal of Marine Systems*, *81*(3), 252–259. https://doi.org/10.1016/j.jmarsys.2009.12.020

Borges, A. V., & Abril, G. (2011). Carbon dioxide and methane dynamics in estuaries. In E. Wolanski, & D. S. McLusky (Eds.), *Treatise on estuarine and coastal science* (Vol. 5, pp. 119–161). Waltham: Academic Press. https://doi.org/10.1016/B978-0-12-374711-2.00504-0

Borges, A. V., & Gypens, N. (2010). Carbonate chemistry in the coastal zone responds more strongly to eutrophication than to ocean acidification. *Limnology and Oceanography*, *55*(1), 346–353. https://doi.org/10.4319/lo.2010.55.1.0346

Brenner, H., Braeckman, U., Le Guitton, M., & Meysman, F. J. R. (2016). The impact of sedimentary alkalinity release on the water column CO_2 system in the North Sea. *Biogeosciences*, *13*(3), 841–863. https://doi.org/10.5194/bg-13-841-2016

Brewer, P. G., & Peltzer, E. T. (2009). Limits to marine life. *Science*, *324*(5925), 347–348. https://doi.org/10.1126/science.1170756

Cai, W.-J., Guo, X., Chen, C.-T. A., Dai, M., Zhang, L., Zhai, W., et al. (2008). A comparative overview of weathering intensity and HCO_3^- flux in the world's major rivers with emphasis on the Changjiang, Huanghe, Zhujiang (Pearl) and Mississippi Rivers. *Continental Shelf Research*, *28*(12), 1538–1549. https://doi.org/10.1016/j.csr.2007.10.014

Cai, W.-J., Hu, X., Huang, W.-J., Jiang, L.-Q., Wang, Y., Peng, T.-H., & Zhang, X. (2010). Surface ocean alkalinity distribution in the western North Atlantic Ocean margins. *Journal of Geophysical Research*, *115*, C08014. https://doi.org/10.1029/2009JC005482

Cai, W.-J., Hu, X., Huang, W.-J., Murrell, M. C., Lehrter, J. C., Lohrenz, S. E., et al. (2011). Acidification of subsurface coastal waters enhanced by eutrophication. *Nature Geoscience*, *4*(11), 766–770. https://doi.org/10.1038/ngeo1297

Cai, W.-J., Huang, W.-J., Luther, G. W. III, Pierrot, D., Li, M., Testa, J., et al. (2017). Redox reactions and weak buffering capacity lead to acidification in the Chesapeake Bay. *Nature Communications*, *8*, 369. https://doi.org/10.1038/s41467-017-00417-7

Caldeira, K., & Wickett, M. E. (2003). Oceanography: Anthropogenic carbon and ocean pH. *Nature*, *425*(6956), 365–365. https://doi.org/10.1038/425365a

Carstensen, J., Conley, D. J., Andersen, J. H., & Ærtebjerg, G. (2006). Coastal eutrophication and trend reversal: A Danish case study. *Limnology and Oceanography*, *51*(1part2), 398–408. https://doi.org/10.4319/lo.2006.51.1_part_2.0398

Dickson, A. G. (1990). Thermodynamics of the dissociation of boric acid in synthetic seawater from 273.15 to 318.15 K. *Deep-Sea Research*, *37*(5), 755–766.

Dickson, A. G., Sabine, C. L., & Christian, J. R. (2007). *Guide to best practices for ocean CO_2 measurements*, PICES Special Publication (Vol. 3, 191 pp.). Oak Ridge, TN: carbon dioxide Inf. Anal. Cent.

Doney, S. C. (2010). The growing human footprint on coastal and open-ocean biogeochemistry. *Science*, *328*(5985), 1512–1516. https://doi.org/10.1126/science.1185198

Doney, S. C., Fabry, V. J., Feely, R. A., & Kleypas, J. A. (2009). Ocean acidification: The other CO_2 problem. *Annual Review of Marine Science*, *1*(1), 169–192. https://doi.org/10.1146/annurev.marine.010908.163834

Duarte, C. M., Hendriks, I. E., Moore, T. S., Olsen, Y. S., Steckbauer, A., Ramajo, L., et al. (2013). Is ocean acidification an open-ocean syndrome? Understanding anthropogenic impacts on seawater pH. *Estuaries and Coasts*, *36*(2), 221–236. https://doi.org/10.1007/s12237-013-9594-3

Dupont, S., Ortega-Martinez, O., & Thorndyke, M. (2010). Impact of near future ocean acidification on echinoderms. *Ecotoxicology*, *19*(3), 449–462. https://doi.org/10.1007/s10646-010-0463-6

Dupont, S., & Pörtner, H.-O. (2013). A snapshot of ocean acidification research. *Marine Biology*, *160*(8), 1765–1771. https://doi.org/10.1007/s00227-013-2282-9

Feely, R. A., Sabine, C. L., Hernandez-Ayon, J. M., Ianson, D., & Hales, B. (2008). Evidence for upwelling of corrosive "acidified" water onto the continental shelf. *Science*, *320*(5882), 1490–1492. https://doi.org/10.1126/science.1155676

Fietzke, J., Ragazzola, F., Halfar, J., Dietze, H., Foster, L. C., Hansteen, T. H., et al. (2015). Century-scale trends and seasonality in pH and temperature for shallow zones of the Bering Sea. *PNAS*, *112*(10), 2960–2965. https://doi.org/10.1073/pnas.1419216112

Frankignoulle, M., Abril, G., Borges, A. V., Bourge, I., Canon, C., Delille, B., et al. (1998). Carbon dioxide emission from European estuaries. *Science*, *282*(5388), 434–436. https://doi.org/10.1126/science.282.5388.434

Fransson, A., Chierici, M., Anderson, L. G., Bussmann, I., Kattner, G., Jones, E. P., & Swift, J. H. (2001). The importance of shelf processes for the modification of chemical constituents in the waters of the Eurasian Arctic Ocean: Implication for carbon fluxes. *Continental Shelf Research*, *21*(3), 225–242. https://doi.org/10.1016/S0278-4343(00)00088-1

Hagens, M., Slomp, C. P., Meysman, F. J. R., Seitaj, D., Harlay, J., Borges, A. V., & Middelburg, J. J. (2015). Biogeochemical processes and buffering capacity concurrently affect acidification in a seasonally hypoxic coastal marine basin. *Biogeosciences*, *12*(5), 1561–1583. https://doi.org/10.5194/bg-12-1561-2015

Havenhand, J. N. (2012). How will ocean acidification affect Baltic Sea ecosystems? An assessment of plausible impacts on key functional groups. *Ambio*, *41*(6), 637–644. https://doi.org/10.1007/s13280-012-0326-x

Hjalmarsson, S., Wesslander, K., Anderson, L. G., Omstedt, A., Perttilä, M., & Mintrop, L. (2008). Distribution, long-term development and mass balance calculation of total alkalinity in the Baltic Sea. *Continental Shelf Research*, *28*(4–5), 593–601. https://doi.org/10.1016/j.csr.2007.11.010

Hu, X., Pollack, J. B., McCutcheon, M. R., Montagna, P. A., & Ouyang, Z. (2015). Long-term alkalinity decrease and acidification of estuaries in northwestern Gulf of Mexico. *Environmental Science & Technology*, *49*(6), 3401–3409. https://doi.org/10.1021/es505945p

Jørgensen, B. B., & Sørensen, J. (1985). Seasonal cycles of O_2, NO_3^- and SO_4^{2-} reduction in estuarine sediments: The significance of an NO_3^- reduction maximum in spring. *Marine Ecology Progress Series*, *24*, 65–74. https://doi.org/10.3354/meps024065

Josefson, A. B., & Rasmussen, B. (2000). Nutrient retention by benthic macrofaunal biomass of Danish estuaries: Importance of nutrient load and residence time. *Estuarine, Coastal and Shelf Science*, *50*(2), 205–216. https://doi.org/10.1006/ecss.1999.0562

Josefson, A. B., & Rasmussen, B. (2004). Species richness of benthic macrofauna in Danish estuaries and coastal areas. *Global Ecology and Biogeography*, *13*, 273–288.

Kemp, W. M., Boynton, W. R., Adolf, J. E., Boesch, D. F., Boicourt, W. C., Brush, G., et al. (2005). Eutrophication of Chesapeake Bay: Historical trends and ecological interactions. *Marine Ecology Progress Series*, *303*, 1–29. https://doi.org/10.3354/meps303001

Le Quéré, C., Andrew, R. M., Canadell, J. G., Sitch, S., Korsbakken, J. I., Peters, G. P., et al. (2016). Global carbon budget 2016. *Earth System Science Data*, *8*(2), 605–649. https://doi.org/10.5194/essd-8-605-2016

Liescka, S., & Riebesell, U. (2012). Synergistic effects of ocean acidification and warming on overwintering pteropods in the Arctic. *Global Change Biology*, *18*(12), 3517–3528. https://doi.org/10.1111/gcb.12020

Melzner, F., Gutowska, M. A., Langenbuch, M., Dupont, S., Lucassen, M., Thorndyke, M. C., et al. (2009). Physiological basis for high CO_2 tolerance in marine ectothermic animals: Preadaptation through lifestyle and ontogeny? *Biogeosciences*, *6*(10), 2313–2331. https://doi.org/10.5194/bg-6-2313-2009

Melzner, F., Thomsen, J., Koeve, W., Oschlies, A., Gutowska, M. A., Bange, H. W., et al. (2013). Future ocean acidification will be amplified by hypoxia in coastal habitats. *Marine Biology*, *160*(8), 1875–1888. https://doi.org/10.1007/s00227-012-1954-1

Millero, F. J. (1986). The pH of estuarine waters. *Limnology and Oceanography*, *31*(4), 839–847. https://doi.org/10.4319/lo.1986.31.4.0839

Millero, F. J. (1995). Thermodynamics of the carbon dioxide system in the ocean. *Geochimica et Cosmochimica Acta*, *59*(4), 661–677.

Millero, F. J., Graham, T. B., Huang, F., Bustos-Serrano, H., & Pierrot, D. (2006). Dissociation constants of carbonic acid in seawater as a function of salinity and temperature. *Marine Chemistry*, *100*(1-2), 80–94. https://doi.org/10.1016/J.MARCHEM.2005.12.001

Mucci, A. (1983). The solubility of calcite and aragonite in seawater at various salinities, temperatures, and one atmosphere total pressure. *American Journal of Science*, *283*, 781–799.

Müller, J. D., Schneider, B., & Rehder, G. (2016). Long-term alkalinity trends in the Baltic Sea and their implications for CO_2-induced acidification. *Limnology and Oceanography*, *61*(6), 1984–2002. https://doi.org/10.1002/lno.10349

Nixon, S. (2009). Eutrophication and the macroscope. *Hydrobiologia*, *629*(1), 5–19. https://doi.org/10.1007/s10750-009-9759-z

Olafsson, J., Olafsdottir, S. R., Benoit-Cattin, A., Danielsen, M., Arnarson, T. S., & Takahashi, T. (2009). Rate of Iceland Sea acidification from time series measurements. *Biogeosciences*, *6*(11), 2661–2668. https://doi.org/10.5194/bg-6-2661-2009

Omstedt, A., Edman, M., Claremar, B., & Rutgersson, A. (2015). Modelling the contributions to marine acidification from deposited SO_x, NO_x, and NH_x in the Baltic Sea: Past and present situations. *Continental Shelf Research*, *111*, 234–249. https://doi.org/10.1016/j.csr.2015.08.024

Orr, J. C., Fabry, V. J., Aumont, O., Bopp, L., Doney, S. C., Feely, R. A., et al. (2005). Anthropogenic ocean acidification over the twenty-first century and its impact on calcifying organisms. *Nature*, *437*(7059), 681–686. https://doi.org/10.1038/nature04095

Petersen, J. K., Hansen, J. W., Laursen, M. B., Clausen, P., Carstensen, J., & Conley, D. J. (2008). Regime shift in a coastal marine ecosystem. *Ecological Applications*, *18*(2), 497–510. https://doi.org/10.1890/07-0752.1

Pierrot, D., E. Lewis, D. W. R. Wallace (2006). MS Excel program developed for CO_2 system calculations, ORNL/CDIAC-105. Oak Ridge, TN: Carbon Dioxide Information Analysis Center, Oak Ridge National Laboratory, U.S. Department of Energy.

Provoost, P., van Heuven, S., Soetaert, K., Laane, R. W. P. M., & Middelburg, J. J. (2010). Seasonal and long-term changes in pH in the Dutch coastal zone. *Biogeosciences*, *7*(11), 3869–3878. https://doi.org/10.5194/bg-7-3869-2010

Reed, D. C., Gustafsson, B. G., & Slomp, C. P. (2016). Shelf-to-basin iron shuttling enhances vivianite formation in deep Baltic Sea sediments. *Earth and Planetary Science Letters*, *434*, 241–251. https://doi.org/10.1016/j.epsl.2015.11.033

Reimer, J. J., Wang, H., Vargas, R., & Cai, W.-J. (2017). Multidecadal fCO_2 increase along the United States southeast coastal margin. *Journal of Geophysical Research: Oceans*, *122*, 10,061–10,072. https://doi.org/10.1002/2017JC013170

Riemann, B., Carstensen, J., Dahl, K., Fossing, H., Hansen, J. W., Jakobsen, H. H., et al. (2016). Recovery of Danish coastal ecosystems after reductions in nutrient loading: A holistic ecosystem approach. *Estuaries and Coasts*, *39*(1), 82–97. https://doi.org/10.1007/s12237-015-9980-0

Ries, J. B., Cohen, A. L., & McCorkle, D. C. (2009). Marine calcifiers exhibit mixed responses to CO_2-induced ocean acidification. *Geology*, *37*(12), 1131–1134. https://doi.org/10.1130/G30210A.1

Saderne, V., Fietzek, P., & Herman, P. M. J. (2013). Extreme variations of pCO_2 and pH in a macrophyte meadow of the Baltic Sea in summer: Evidence of the effect of photosynthesis and local upwelling. *PLoS One*, *8*(4), e62689. https://doi.org/10.1371/journal.pone.0062689

Soetart, K., Middelburg, J. J., Heip, C., Meire, P., van Damme, S., & Maris, T. (2006). Long-term change in dissolved inorganic nutrients in the heterotrophic Scheldt estuary (Belgium, the Netherlands). *Limnology and Oceanography*, *51*(1part2), 409–423. https://doi.org/10.4319/lo.2006.51.1_part_2.0409

Spilling, K., Schulz, K. G., Paul, A. J., Boxhammer, T., Achterberg, E. P., Hornick, T., et al. (2016). Effects of ocean acidification on pelagic carbon fluxes in a mesocosm experiment. *Biogeosciences*, *13*(21), 6081–6093. https://doi.org/10.5194/bg-13-6081-2016

Thomas, H., Schiettecatte, L. S., Suykens, K., Koné, Y. J. M., Shadwick, E. H., Prowe, F., et al. (2009). Enhanced ocean carbon storage from anaerobic alkalinity generation in coastal sediments. *Biogeosciences*, *6*(2), 267–274. https://doi.org/10.5194/bg-6-267-2009

Thomsen, J., Gutowska, M. A., Saphörster, J., Heinemann, A., Trübenbach, K., Fietzke, J., et al. (2010). Calcifying invertebrates succeed in a naturally CO_2-rich coastal habitat but are threatened by high levels of future acidification. *Biogeosciences*, *7*(11), 3879–3891. https://doi.org/10.5194/bg-7-3879-2010

Tyrrell, T., Schneider, B., Charalampopoulou, A., & Riebesell, U. (2008). Coccolithophores and calcite saturation state in the Baltic and Black Seas. *Biogeosciences*, *5*(2), 485–494. https://doi.org/10.5194/bg-5-485-2008

Ulfsbo, A., Kuliński, K., Anderson, L. G., & Turner, D. R. (2015). Modelling organic alkalinity in the Baltic Sea using a Humic-Pitzer approach. *Marine Chemistry*, *168*, 18–26. https://doi.org/10.1016/j.marchem.2014.10.013

Waldbusser, G. G., Powell, E. N., & Mann, R. (2013). Ecosystem effects of shell aggregations and cycling in coastal waters: An example of Chesapeake Bay oyster reefs. *Ecology*, *94*(4), 895–903. https://doi.org/10.1890/12-1179.1

Waldbusser, G. G., Voigt, E. P., Bergschneider, H., Green, M. A., & Newell, R. I. (2011). Biocalcification in the eastern oyster (*Crassostrea virginica*) in relation to long-term trends in Chesapeake Bay pH. *Estuaries and Coasts*, *34*(2), 221–231. https://doi.org/10.1007/s12237-010-9307-0

Weiss, R. F. (1974). Carbon dioxide in water and seawater: The solubility of a non-ideal gas. *Marine Chemistry*, *2*(3), 203–215. https://doi.org/10.1016/0304-4203(74)90015-2

Wolf-Gladrow, D. A., Zeebe, R. E., Klaas, C., Körtzinger, A., & Dickson, A. G. (2007). Total alkalinity: The explicit conservative expression and its application to biogeochemical processes. *Marine Chemistry*, *106*(1-2), 287–300. https://doi.org/10.1016/j.marchem.2007.01.006